

1 **Insights into the phylogenetic position and phylogeography of the monospecific skink-**  
2 **parasite genus *Neoentomelas* (Nematoda : Rhabditida : Rhabdiasidae), with special**  
3 **reference to the effects of the reproductive mode on the genetic diversity**

4  
5 *Naoya Sata*<sup>A,B,C</sup> and *Takafumi Nakano*<sup>B</sup>

6  
7 <sup>A</sup>Meguro Parasitological Museum, Meguro-ku, Tokyo 153-0064, Japan.

8 <sup>B</sup>Department of Zoology, Graduate School of Science, Kyoto University, Sakyo-ku, Kyoto  
9 606-8502, Japan.

10 <sup>C</sup>Corresponding author. Email: nsata@kiseichu.org

11

12 RT: Phylogeny and genetic diversity of *Neoentomelas*

13

14 **Short summary** ( $\leq 60$  words, jargon free)

15 *Neoentomelas asatoi* is a parasitic nematode that infests only a scincid lizard species in  
16 Ryukyu Archipelago, Japan. We clarified the phylogenetic distinctiveness of *Neoentomelas* in  
17 Rhabdiasidae, and revealed at least three dispersal events of the major clades within *N. asatoi*.  
18 Our results provide new insight into the evolutionary history of Rhabdiasidae and the  
19 diversification factors of parasites.

20

21 **Abstract.** *Neoentomelas asatoi* Hasegawa, 1989 is a parasitic nematode that infests only the  
22 scincid lizard *Ateuchosaurus pellopleurus* (Hallowell, 1861), which inhabits the forest floor in  
23 Northern and Central Ryukyu Archipelago, Japan. As a member of Rhabdiasidae, the  
24 reproductive mode of *N. asatoi* is characterized by the alternation of the protandrous  
25 hermaphroditic mode and gonochoristic mode throughout its life cycle. The intrafamily  
26 phylogenetic position and intraspecific diversity of this nematode species were inferred by  
27 molecular phylogenetic analyses. The results revealed the phylogenetic distinctiveness of  
28 *Neoentomelas* Hasegawa, 1989 in Rhabdiasidae, which supports the unique generic status of  
29 *Neoentomelas* within the family. The intraspecific phylogenetic analyses of *N. asatoi* revealed  
30 a minor concordant phylogenetic pattern with the host and mosaic geographic arrangement of  
31 the major clades, which was discordant with the host. The analyses and distribution pattern of  
32 subclades suggested that this geographic arrangement can be explained by at least three  
33 dispersal events and subsequent switching to indigenous host populations. Colonization  
34 events might be promoted by the high establishment rate of new populations stemming from  
35 the parthenogenesis-like reproduction mode of *N. asatoi*. The present study demonstrated that  
36 reproductive modes can affect the intraspecific genetic diversity of parasites.

37

38 **Additional keywords:** *Ateuchosaurus pellopleurus*, endoparasite, Japan, Ryukyu  
39 Archipelago

40

## 41 **Introduction**

42

43 Vicariance events of host species and host-switching events of parasites are essential for the  
44 formation of diversification and distribution patterns of parasites (Koehler *et al.* 2009; Badets  
45 *et al.* 2011; Sands *et al.* 2017). The dispersal ability of organisms influences their intraspecific  
46 genetic diversity and speciation rate (Peterson and Denno 1998; Kisel and Barraclough 2010;  
47 Ikeda *et al.* 2012): low dispersal ability leads to a low rate of gene flow and promotes  
48 interpopulation genetic divergence, and high dispersal ability leads to a high rate of gene flow  
49 and suppresses interpopulation genetic divergence. Therefore, the mobility of hosts and host  
50 richness (the number of possible host taxa) are the major determinants of the dispersal ability  
51 of parasites (e.g., Blasco-Costa and Poulin 2013; Falk and Perkins 2013), and the vicariance  
52 of the host population would serve as barriers for the interpopulation gene flow of parasites  
53 that have sedentary hosts or narrow host ranges. In this case, cophylogenetic patterns would  
54 be expected between hosts and parasites. However, many previous studies have reported  
55 discrepant phylogenetic and distribution patterns between hosts and parasites, which have  
56 sedentary hosts or narrow host ranges at various scales; such discrepancies are speculated to  
57 be the result of asymmetric geographic range expansion and/or host switching events (e.g.,  
58 Wickstöm *et al.* 2003; Haukisalmi *et al.* 2016). Thus, it is important to determine the degree  
59 of diversification pattern of parasites that can be explained by host divergence or host  
60 switching to improve our knowledge of the diversification factors of parasites. Comparative  
61 phylogeographic studies on certain hosts and parasites are useful to determine which  
62 phylogeographic events have occurred.

63 The Ryukyu Archipelago, which consists of three parts—the Northern, Central and  
64 Southern Ryukyus, is located between the Japanese main islands and Taiwan (Fig. 1).  
65 Previous systematic and phylogeographic studies have revealed great specific and  
66 genetic diversity of reptiles in this archipelago (Ota 1998; Okamoto 2017). These studies  
67 also pointed out the high endemism of reptilian fauna in Central Ryukyus (Ota 1998;  
68 Okamoto 2017), and thus, these putative host species can be expected to harbor diverse  
69 and unique parasites. In contrast to our knowledge about the endemism and  
70 phylogeographic features of reptiles inhabiting the Ryukyu Archipelago, little is known  
71 about the diversity and diversification process of parasites in the reptiles distributed in  
72 this area (but also see Hasegawa and Iwatsuki 1984; Hasegawa 1985).

73 The rhabdiasid *Neoentomelas* Hasegawa, 1989 is a monospecific nematode genus  
74 known from Ryukyu Archipelago, which contains only the species *Neoentomelas asatoi*

75 Hasegawa, 1989. Recent studies have clarified that rhabdiasid genera exhibit certain host  
76 specificity (Kuzmin and Tkach 2011; Kuzmin 2013; Tkach *et al.* 2014); *N. asatoi* also  
77 exhibits strict host specificity and only infects the lung of the scincid lizard  
78 *Ateuchosaurus pellopleurus* (Hallowell, 1861), which inhabits the forest floor throughout  
79 Central Ryukyus and part of Northern Ryukyus (Hasegawa 1989, 1990, 1992; Sata  
80 2015). Morphological and phylogeographic studies have suggested the endemism of *A.*  
81 *pellopleurus* in Central Ryukyus and its recent range expansion from Central Ryukyus to  
82 Northern Ryukyus (Ota *et al.* 1999; Makino *et al.* 2020). A molecular phylogenetic study  
83 also revealed the deep genetic divergence between the Okinawa Islands population and  
84 the Amami Islands to the northern Ryukyus population (Makino *et al.* 2020).

85 The known geographic range of *N. asatoi* covers most of the geographic range of *A.*  
86 *pellopleurus*: Amamioshima Island, Okinawajima Island, and Kumejima Island  
87 (Hasegawa 1989, 1990, 1992). Although the life cycle of this nematode has not been  
88 elucidated, all investigated rhabdiasid species require no intermediate host in their life  
89 cycle. The life cycle of most rhabdiasid species is characterized by the alternation of  
90 parasitic and free-living generations; the former is reproduced by a protandrous  
91 hermaphroditic mode, and the latter is reproduced by a gonochoristic mode (Anderson  
92 2000; Kuzmin 2013). Protandrous hermaphroditism requires only a single individual for  
93 reproduction and can allow single individuals to establish new populations, such as in  
94 parthenogenesis. Hence, it is estimated that *N. asatoi* has a high success rate of new-  
95 population establishment, and thus its phylogeographic pattern is affected by its  
96 reproductive mode. Accordingly, the comparison of phylogeographic patterns of *N.*  
97 *asatoi* with *A. pellopleurus* is essential for improving our understanding of the  
98 diversification process of parasites reproduced by the parthenogenesis-like mode.

99 Rhabdiasidae currently comprises eight genera, and most of the species dwell in the  
100 lungs of reptiles or amphibians (Kuzmin 2013; Tkach *et al.* 2014). Several authors  
101 predicted that *Neoentomelas* and *Kurilonema* Shcherbak & Sharpilo, 1969 share the  
102 most recent common ancestor because they have highly similar morphological and  
103 ecological features, i.e., both genera possess ‘a large buccal capsule with a chitinized  
104 wall’, and their host ranges are mostly limited to scincid lizards (Shcherbak and Sharpilo  
105 1969; Hasegawa 1989, 1990, 1992; Telford 1997; Bursey *et al.* 2005; Sata 2015).  
106 Additionally, *Entomelas* Travassos, 1930 and *Kurilonema* also share morphological  
107 features, including a large buccal capsule with a chitinized wall, and are distinguished  
108 from each other only by the characteristics of teeth in the bottom of the buccal capsule;

109 *Entomelas* possesses teeth, while *Kurilonema* lacks teeth (Baker 1980; Kuzmin and  
110 Sharpilo 2002). The morphological similarities among these genera lead to arguments  
111 about the validity of their taxonomic status as a distinct genus (Baker 1980; Kuzmin and  
112 Sharpilo 2002). Therefore, systematic accounts of *Neoentomelas*, *Kurilonema* and  
113 *Entomelas* should be elucidated to elucidate the evolutionary history of these rhabdiasid  
114 genera.

115 In the present study, we aim to clarify the systematic accounts of *Neoentomelas*,  
116 *Kurilonema*, and *Entomelas* as distinct genera by inferring the intrafamily phylogenetic  
117 relationship of Rhabdiasidae with molecular phylogenetic analyses based on nuclear  
118 DNA sequences. We also aimed to elucidate whether the interspecific genetic  
119 diversification pattern of *N. asatoi* deviates from the phylogeographic pattern of *A.*  
120 *pellopleurus* by comparing the intraspecific phylogenetic pattern inferred from  
121 mitochondrial and nuclear DNA sequences with the molecular phylogenetic tree of *A.*  
122 *pellopleurus* estimated by Makino *et al.* (2020). Accordingly, we reinforce the taxonomic  
123 stability of rhabdiasid nematodes and provide new insight into diversification factors of  
124 parasites.

125

## 126 **Materials and methods**

### 127 *Sampling*

128 From 2014 to 2018, a total of 123 individuals of *A. pellopleurus* were collected from 21  
129 localities on 15 islands of Central and Northern Ryukyus (Fig. 1). Hosts were euthanized by  
130 oral injection with sodium pentobarbital and then dissected. The euthanized hosts were stored  
131 at  $-80^{\circ}\text{C}$  until dissection. Their lungs were examined under a stereoscopic microscope  
132 (model Eclipse Ni-U, Nikon, Tokyo, Japan); nematodes were collected when they were  
133 present in the lungs. The nematodes obtained were fixed in hot 70% glycerin ethanol, cleared  
134 in 100% glycerin, and morphologically identified to species. The identified specimens were  
135 preserved in 70% ethanol at  $-20^{\circ}\text{C}$  until DNA extraction. The locality names where *N. asatoi*  
136 was collected are listed in Table 1. We also collected *Kurilonema markovi* Shcherbak &  
137 Sharpilo, 1969 (Rhabdiasidae) from *Plestiodon* Duméril & Bibron, 1839 lizards as additional  
138 operational taxonomic units for intrafamily phylogenetic inference and as outgroups for  
139 intraspecific phylogenetic inference. The details of the parasitic record will be described in  
140 future papers. All hosts were collected and handled in accordance with the Regulations of  
141 Animal Experimentations at Kyoto University (approval numbers: H24014, H2711).

142 Several representative specimens of *N. asatoi* (KUZ Z2731–Z2750; Table S1) and all

143 lizard specimens examined in this study were deposited in the Zoological Collection of Kyoto  
144 University (KUZ) as the voucher specimens of this study.

145

#### 146 *DNA sequencing*

147 We used 74 specimens of *N. asatoi* for molecular phylogenetic analyses. Genomic DNA was  
148 extracted from each specimen following the method described by Sata (2018). Two fragments  
149 of mitochondrial DNA, cytochrome *c* oxidase subunit I (*COI*) and 12S ribosomal DNA (*I2S*),  
150 and nuclear DNA fragments, including the 3' end of 18S rDNA, internal transcribed spacer  
151 (*ITS*) 1, 5.8S rDNA, ITS 2, and the 5' end of 28S rDNA (*I8S–28S*), were amplified by  
152 polymerase chain reaction (PCR) using a TaKaRa Ex Taq kit (Takara Bio Inc., Kusatsu,  
153 Japan) and GeneAmp PCR Systems 2700 or 9700 (Thermo Fisher Scientific, Waltham, MA,  
154 USA). The primer sets and PCR conditions for amplifications followed Prosser *et al.* (2013)  
155 for *COI*, Casiraghi *et al.* (2004) for *I2S*, and Tkach *et al.* (2014) for *I8S–28S*. We also used a  
156 newly designed primer (nkITSf: 5'-ACCGGGTAAAAGTCGTAACAAG-3') instead of a  
157 'rift', which is a forward primer used in Tkach *et al.* (2014), for the forward primer to amplify  
158 *I8S–28S* under modified PCR conditions.

159 The PCR products were purified with ExoSAP-IT reagent (Thermo Fisher Scientific).  
160 Sequencing reactions were performed using a BigDye Terminator Cycle Sequencing Kit (ver.  
161 3.1, Thermo Fisher Scientific) with the primers described in Messing (1983) for *COI* (M13F  
162 and M13R); the primers corresponded to those used for PCR for *I2S*; and the primers  
163 described by Tkach *et al.* (2014) and newly designed primers, nkITSf, nkf01 (5'-  
164 GCATATCAGTAAGCGGAGGA-3'), nkf02 (5'-AAACACGGACCAAGGAGTCTAG-3'),  
165 and nkr01 (5'-TCCTCCGCTTACTGATATGC-3') for *I8S–28S*. The products were cleaned by  
166 ethanol precipitation and sequenced using an Applied Biosystems 3130xl Genetic Analyzer  
167 (Thermo Fisher Scientific). All determined sequences were deposited with the DNA Data  
168 Bank of Japan (*COI*: LC632082–LC632157; *I2S*: LC632158–LC632226; *I8S–28S*:  
169 LC631491–LC631542).

170

#### 171 *Phylogenetic inferences*

172 Phylogenetic trees were reconstructed using maximum likelihood (ML) and Bayesian  
173 inference (BI) based on both datasets of nuclear (for the intrafamily relationship of  
174 Rhabdiasidae) and mitochondrial DNA sequences (for the intraspecific relationship of *N.*  
175 *asatoi*).

176 1. The phylogenetic position of *Neoentomelas* and other related genera was estimated

177 based on 18S–28S sequences. In total, 44 rhabdiasid operational taxonomic units (OTUs)  
178 were included (i.e., two *Neoentomelas*, three *Kurilonema*, six *Serpentirhabdias*, five  
179 *Entomelas*, three *Pneumonema* and 30 *Rhabdias* OTUs) (Tables S2 and S3). The sequences  
180 were edited with MEGA 5 (Tamura *et al.* 2011) and aligned with MAFFT L-INS-i (ver. 7.427,  
181 see <https://mafft.cbrc.jp/alignment/software/>; Katoh and Standley 2013). Regions difficult to  
182 align because of alignment gaps were removed manually; thus, the final sequences yielded  
183 2084 bp of aligned positions for 18S–28S. The best-fit partition scheme and models were  
184 identified based on the corrected Akaike information criterion (AICc) using PartitionFinder  
185 (ver. 2.1.1, see <http://www.robertlanfear.com/partitionfinder/>; Lanfear *et al.* 2017) with the  
186 ‘all’ algorithm: for 18S and 5.8S, GTR+G; for ITS 1, GTR+I+G; for ITS 2, GTR+I+G; and  
187 for 28S, GTR+G. The ML phylogenetic tree was calculated using IQ-TREE (ver. 2.1.3, see  
188 <http://www.iqtree.org/>; Minh *et al.* 2020) with nonparametric bootstrapping (BS) conducted  
189 with 1000 replicates. BI tree and Bayesian posterior probabilities (PP) were estimated using  
190 MrBayes (ver. 3.2.7a, see <https://nbisweden.github.io/MrBayes/download.html>; Ronquist *et al.*  
191 *et al.* 2012). Two independent runs for four Markov chains were conducted for 1 million  
192 generations, and the tree was sampled every 100 generations. The parameter estimates and  
193 convergence were checked using Tracer (ver. 1.7.1, see  
194 <http://tree.bio.ed.ac.uk/software/tracer/>; Rambaut *et al.* 2018), and the first 2501 trees were  
195 discarded based on the results.

196 2. The phylogenetic relationships within the available *N. asatoi* samples were estimated  
197 based on *COI* and *12S* sequences. The mitochondrial (sequences of all loci were  
198 concatenated) dataset was collapsed to only those with unique mtDNA haplotypes  
199 (individuals possessing identical sequences in the sequenced loci were treated as those with  
200 the same haplotype, even if some of them had missing loci). In total, 37 *N. asatoi* OTUs were  
201 included as ingroup taxa (Tables 1, S2). The sequences were edited with MEGA 5 and aligned  
202 with Clustal W (Thompson *et al.* 1994) for *COI* and MAFFT L-INS-i for *12S*. Regions  
203 difficult to align because of alignment gaps were removed manually for *12S*; thus, the final  
204 sequences yielded 655 bp of aligned positions for *COI* and 528 bp for *12S*. The best-fit  
205 partition scheme and models were identified based on AICc using PartitionFinder with the  
206 ‘all’ algorithm. The selected partition scheme and models were as follows: for the *COI* 1st  
207 position, GTR+G; for the *COI* 2nd position, GTR; for the *COI* 3rd position, HKY+G; for *12S*,  
208 HKY+G. The ML phylogenetic tree was also calculated using IQ-TREE with nonparametric  
209 BS conducted with 1000 replicates. BI tree and Bayesian PP were estimated using MrBayes;  
210 two independent runs for four Markov chains were conducted for 2 million generations, and

211 the tree was sampled every 100 generations. The parameter estimates and convergence were  
212 checked using Tracer, and the first 5001 trees were discarded based on the results.

213 3. The haplotype relationships within the available *N. asatoi* samples were estimated  
214 based on *18S–28S* sequences. In total, 47 *N. asatoi* OTUs were included as ingroup taxa  
215 (Tables 1, S2). The sequences were edited with MEGA 5 and aligned with Clustal W, and the  
216 final sequences yielded 1441 bp of aligned positions. The haplotype relationships of *18S–28S*  
217 were inferred by statistical parsimony with the TCS (Clement *et al.* 2000) algorithm  
218 implemented in PopART (ver. 1.7, see <http://popart.otago.ac.nz/index.shtml>; Leigh and  
219 Bryant 2015).

220

## 221 **Results**

### 222 *Sequencing*

223 We successfully sequenced 615–655 bp of *COI* for 74 specimens of *N. asatoi*, 521–528 bp of  
224 *12S* for 68 specimens, and 1371–2123 bp of *18S–28S* for 50 specimens. Unfortunately, the  
225 sequence quality of the *18S–28S* sequence of Clade I (see below) was too poor, which can be  
226 ascribed to the slippage of Taq DNA polymerase at a poly-T region. The haplotype  
227 compositions at each island are shown in Table 1.

228

### 229 *Intrafamily phylogenetic relationship*

230 Both ML and BI phylogenetic inference based on the *18S–28S* DNA sequence dataset yielded  
231 almost identical topologies; thus, the BI tree with BI and ML support values is shown in Fig.  
232 2. Phylogenetic inference reconstructed each of the six rhabdiasid genera as distinct clades.  
233 The sister relationship between *Neoentomelas* and *Kurilonema* was strongly supported by  
234 both analyses (PP = 1.0; BP = 89%). The monophyly of *Entomelas* + *Rhabdias* +  
235 *Pneumonema* was also strongly supported by both analyses (PP = 0.99; BP = 91%). The  
236 monophyly of *Neoentomelas* + *Kurilonema* and *Entomelas* was not supported by the present  
237 inference, and the sister clade of the *Entomelas* clade could not be clarified by the present  
238 datasets.

239

### 240 *Intraspecific phylogenetic relationship*

241 Both ML and BI phylogenetic inference based on the *COI* and *12S* DNA sequence datasets  
242 yielded mostly identical topologies; thus, the BI tree with BI and ML support values is shown  
243 in Fig. 3. Phylogenetic inference reconstructed three major clades, Clades I, II, and III. Clade  
244 I occurs only on Kumejima Island (haplotype K1), and Clade II occurs only on Tokunoshima



245 Island (haplotypes Tku1, 2). Clade III consisted of seven subclades: subclade Mishima  
246 (occurring on the Iou and Takeshima Islands; haplotypes M1, 2), subclade Tokara (occurring  
247 on Suwanosejima and Kodakarajima Islands; haplotypes T1–T3), subclade Okinawa  
248 (occurring on Okinawajima Island; haplotypes O1–O3), subclade Tokashiki (occurring on  
249 Tokashikijima Island; haplotypes Tka1, 2), subclade Hamahiga (occurring on Hamahigalima  
250 Island; haplotype Hm1), subclade Kume (occurring on Kumejima Island; haplotypes K2–K6);  
251 and subclade Iheya–Amami (occurring on Iheyajima and Amamioshima Islands; haplotypes  
252 I1–I4, Aa1–5, and Ay1–Ay9). The populations that occurred on the Islands of Iheyajima and  
253 Amamioshima were composed of a single clade (PP = 0.94; BP = 64%), although they were  
254 located on different groups of islands: Iheyajima Island was grouped into the Okinawa  
255 Islands, and Amamioshima Island was grouped into the Amami Islands. Furthermore, the  
256 present analyses strongly supported the sister relationship between subclade Tokara  
257 (occurring in northern Ryukyus and southern Tokara Islands) and subclade Okinawa  
258 (occurring in the Okinawa Islands) in Clade III (PP = 0.91; BP = 72%). Kumejima Island  
259 accommodated two deeply diverged lineages, one belonging to Clade I and another to Clade  
260 III.

261

#### 262 *Statistical parsimony network*

263 The statistical parsimony network of 57 haplotypes of 18S–28S is shown in Fig. 4. In this  
264 network, two distinct clusters separated by four steps were recognized (A and B in Fig. 4).  
265 The two haplotypes (H4 and H5) of Cluster A occurred only on Tokunoshima Island, and the  
266 other six haplotypes (H1–H3 and H6–H8) of Cluster B occurred on the remaining islands. In  
267 the Iheyajima and Amami Islands, a single identical haplotype (H6) was shared. This  
268 haplotype was also detected in Ogimi Village, Okinawajima Island. Although the haplotype  
269 that occurred on Kodakarajima Island was identified as H6, this sequence was distinguished  
270 from ‘true’ H6 by a single indel-derived polymorphism.

271

## 272 **Discussion**

### 273 *Phylogenetic position of Neoentomelas and taxonomic implications*

274 Our phylogenies revealed that three genera, *Neoentomelas*, *Kurilonema* and *Entomelas*,  
275 represent distinct monophyletic groups, and *Neoentomelas* form sister clades of *Kurilonema*.  
276 Several previous studies predicted the close relationship of *Neoentomelas* and *Kurilonema*, as  
277 they possess noticeable morphological and ecological similarities (Hasegawa 1989; Kuzmin  
278 and Sharpilo 2002; Kuzmin and Tkach 2011). The present results provide the first molecular

279 phylogenetic support for the close relationship between the two genera, and their shared  
280 morphological characteristics, a large buccal capsule with a chitinized wall, can be regarded  
281 as a synapomorphy. However, because they exhibit certain genetic and morphological (well-  
282 developed dorsoventral lips in *Neoentomelas* vs. small lips in *Kurilonema*) differences, each  
283 taxon might be treated as a distinct genus. Accordingly, the possession of a large buccal  
284 capsule with a chitinized wall should be regarded as a synapomorphy for the *Neoentomelas*  
285 and *Kurilonema* clades.

286 The known host range of *Neoentomelas* is restricted to *A. pellopleurus* (Hasegawa 1989,  
287 1990, 1992), and *Kurilonema* are mainly *Plestiodon* (in Japan) (Shcherbak and Sharpilo 1969;  
288 Telford 1997; Bursey *et al.* 2005; Sata 2015) and *Pinoyscincus* Linkem, Diesmos & Brown,  
289 2011 (in the Philippines) (formerly *Sphenomorphus* Fitzinger, 1843; see Linkem *et al.* 2011)  
290 lizards (Kuzmin and Tkach 2011). *Ateuchosaurus* and *Pinoyscincus* belong to Lygosominae  
291 in Scincidae and *Plestiodon* to Scincinae in Scincidae (Greer and Shea 2000; Pyron *et al.*  
292 2013; Makino *et al.* 2020). Given the current host ranges of *Neoentomelas* and *Kurilonema*,  
293 the host of the most recent common ancestor of these two genera should be scincid lizards.

294 Our results did not support the monophyly of *Kurilonema* and *Entomelas*. These species  
295 exhibit high morphological similarity and are distinguished from each other only by the  
296 presence or absence of teeth at the bottom of the buccal cavity (Shcherbak and Sharpilo 1969;  
297 Baker 1980; Kuzmin and Sharpilo 2002). Baker (1980) regarded the presence or absence of  
298 teeth as insufficient to propose the genus and synonymized *Kurilonema* with *Entomelas*.  
299 Kuzmin and Sharpilo (2002) emphasized the validity of the morphology of the anterior region  
300 of rhabdiasid nematodes to differentiate their higher taxa and regarded their generic status as  
301 distinct. Our phylogeny supported the distinct taxonomic status of these genera, as indicated  
302 by Kuzmin and Sharpilo (2002), and the presence of teeth should be a synapomorphy of  
303 *Entomelas*. It is also noteworthy that they differ in their host usages, i.e., *Kurilonema* species  
304 mainly utilize Scincidae lizards, and *Entomelas* species mainly utilize Anguinae lizards as  
305 hosts (Kuzmin 2013). Furthermore, since our phylogeny did not support the monophyly of the  
306 *Neoentomelas* + *Kurilonema* clade and *Entomelas*, the apparent sharing of close  
307 morphological features, i.e., the large buccal capsule with a chitinized wall, between  
308 *Kurilonema* and *Entomelas* may have arisen independently.

309

### 310 *Phylogeography of Neoentomelas asatoi*

311 The present intraspecific phylogenetic analysis based on the mitochondrial DNA sequences  
312 revealed three major clades (Clades I–III). Clades II and III could also be recognized as

313 Clusters A and B by the *18S–28S* haplotypes. These three clads showed mosaic geographic  
314 arrangement. Clades I and II occurred only on Kumejima Island and Tokunoshima Island,  
315 respectively, and Clade III occurred in all studied areas except Tokunoshima Island. Given  
316 that *N. asatoi* was originally described from Okinawajima Island, a monophyletic group  
317 comprising Clades II and III should represent the ‘true’ *N. asatoi*. Future detailed  
318 morphological and genetic analyses are desired to reveal the taxonomic status of Clade III.

319 All subclades occurring in the Okinawa Islands, except one subclade occurring on  
320 Kumejima Island, clustered into a single clade (Clade III), and this clade deeply diverged  
321 from Clade II, which occurred only on Tokunoshima Island in the Amami Islands. This  
322 pattern is mostly concordant with the host phylogeographic pattern, i.e., the deep allopatric  
323 genetic divergence between Okinawa Islands populations and Amami Islands–northern Ryukyu  
324 Islands populations (Makino *et al.* 2020). Subclades that occurred on Amamioshima Island on  
325 the Amami Islands, Tokara Islands and Mishima Islands were also clustered into Clade III.  
326 This pattern is discordant with the host phylogeography (Fig. 5). To explain this discordant  
327 distribution pattern between *N. asatoi* and *A. pellopleurus*, two modes of phylogeographic  
328 events are possible: (1) range expansions of *N. asatoi* via land bridges without host  
329 colonization followed by vicariance caused by the subsidence of the bridges; and (2) recent  
330 dispersal of *N. asatoi* and subsequent colonization without host colonization.

331 The Ryukyu Archipelago evolved from a continental margin to an island arc. The  
332 paleogeographic history of Central Ryukyus is recognized as follows: (1) Central Ryukyus  
333 was isolated from the surrounding areas by formation of straits in the Pliocene as a land mass;  
334 (2) in the middle Pleistocene, the land mass was divided into several islands due to the  
335 relative increase in sea level; and (3) in the late Pleistocene, land bridges between adjacent  
336 islands were formed due to the relative decrease in sea level. During this period,  
337 Amamioshima Island was connected with other islands in the Amami Islands but not with  
338 islands in the Okinawa Islands. (4) Then, the land bridges subsided due to the relative  
339 increase in sea level, and the present sets of islands in the Amami and Okinawa Islands were  
340 constructed (Osozawa *et al.* 2012; Furukawa and Fujitani 2014). Given the long isolation  
341 history between Amamioshima Island and the Okinawa Islands, the genetic affinity between  
342 the Amamioshima island population in the Amami Islands and the Iheyajima population in the  
343 Okinawa Islands may be explained by the recent colonization of *N. asatoi* without their host  
344 lizard.

345 The mitochondrial phylogenetic relationship between Iheyajima and Amamioshima was  
346 reticulated, and a single haplotype of *18S–28S* was shared by both island populations. The

347 phylogenetic analysis also revealed a sister relationship between subclade Iheya–Amami and  
348 a clade comprising subclade Hamahiga and subclade Kume (both subclades occur on islands  
349 that are members of the Okinawa Islands). Hence, these Okinawa Islands' lineages were  
350 paraphyletic to Amamioshima Island's lineage. The most plausible explanation of these is the  
351 occurrence of the recent colonization of *N. asatoi* from Iheyajima Island to Amamioshima  
352 Island (Fig. 5).

353 Thus, the following scenario would be suggested: (1) Clade II was distributed across the  
354 entire Amami Islands, and (2) invasion of the lineage(s) of Clade III from Iheyajima Island to  
355 Amamioshima Island occurred, and then the Clade II populations were excluded by some  
356 exclusive interaction with the Clade III lineage(s) there.

357 The Tokara Islands are geologically composed of two parts i.e., northern Tokara and  
358 southern Tokara Islands (Fig. 1), and these island groups belong to Northern Ryukyus and  
359 Central Ryukyus, respectively. Northern Ryukyus has been isolated from Central Ryukyus by  
360 a deep strait since the Pliocene. The northern Tokara Islands were formed by submarine  
361 volcanic activity in the middle Pleistocene, when isolation of the island of the Central  
362 Ryukyus began. Additionally, the southern Tokara Islands were formed by submarine volcanic  
363 activity in the early Pleistocene, and they have been isolated from other islands in the Central  
364 Ryukyus (Osozawa *et al.* 2012). Because both northern and southern Tokara Islands have  
365 been isolated from Central Ryukyus for a long time since their emergence, the close genetic  
366 affinities among Suwanosejima Island (northern Tokara Islands), Kodakarajima Island  
367 (southern Tokara Islands), and Okinawajima (Okinawa Islands) Island populations could not  
368 be explained by the range expansions promoted by the emergence of the land bridges and  
369 subsequent vicariant events caused by the submergences of the land bridges, but the recent  
370 colonization of *N. asatoi* without their host lizard. However, the direction of colonization  
371 could not be revealed by the present datasets (Fig. 5). Accordingly, multiple colonization  
372 events, at least three times, can explain the mosaic geographic arrangement of Clade III (Fig.  
373 5).

374 The presence of the unique lineage in the Mishima Islands conflicts with the  
375 phylogeographic history of the host populations, which were established by its recent  
376 northward dispersal (Makino *et al.* 2020). However, we are convinced that further sampling  
377 would clarify their closely related parental population.

378 The present study unveiled that the mosaic geographic arrangement of the intraspecific  
379 lineages of *N. asatoi* could be explained by multiple colonization events. Multiple  
380 colonization events were also reported from the phylogenetic study of *Meteterakis* Karve,

381 1930 (Heterakoidea) nematode species parasitizing the intestinal tract of scincid lizards  
382 (including *A. pelloporeurus*) and frogs in the Ryukyu and Japanese Archipelagos (Sata 2018).  
383 Because *Meteterakis* species exhibit a wide host range and utilize *Plestiodon* lizards, which  
384 experienced multiple overseas dispersal events in the Ryukyu Archipelago, they were  
385 expected to be highly dispersible parasites (Sata 2018). However, since *N. asatoi* utilizes only  
386 a locally diverged small forest-floor dwelling lizard, it is surprising that *N. asatoi* experienced  
387 multiple colonization events, similar to the *Meteterakis* species.

388 Heterakoid species are homoxenous parasites, similar to rhabdiasid species (Anderson  
389 2000). They reproduce only by a gonochoristic mode (Anderson 2000), whereas rhabdiasid  
390 species reproduce by alternation of protandrous hermaphroditic mode and gonochoristic mode  
391 (Anderson 2000; Kuzmin 2013). Protandrous hermaphrodites require only a single individual  
392 for reproduction (i.e., uniparental reproduction), and in that sense, they are equivalent to  
393 parthenogenesis. Generally, parthenogenesis can allow single individuals to establish new  
394 populations. Thus, the multiple colonization events of *N. asatoi* can be ascribed to the high  
395 success rate of new population establishment stemming from parthenogenesis-like  
396 reproduction. The present study suggested that parthenogenesis and parthenogenesis-like  
397 reproduction can promote the population establishment of parasites in new areas and construct  
398 unexpected phylogeographic patterns from the host phylogeographic pattern. Further  
399 comparative phylogeographic studies are needed to evaluate the effect of the heterogonic life  
400 cycle on the population genetic divergence of parasites.

401

#### 402 **Concluding remarks**

403 The present study discussed the taxonomic status of three rhabdiasid genera: *Neoentomelas*,  
404 *Kurilinema*, and *Entomelas*. Each of the three genera was reconstructed as distinct clades.  
405 Thus, our phylogeny supported the distinct generic status of these three genera in  
406 Rhabdiasidae. The mosaic geographic arrangement of the major clades of *N. asatoi* was  
407 clarified, and the intraspecific phylogenetic tree of *N. asatoi* was not completely concordant  
408 with the host tree. This arrangement was explained by at least three colonization events, and  
409 one of them was explained by northward dispersal and subsequent switching to indigenous  
410 host populations. These colonization events might be promoted by the high establishment rate  
411 of new populations stemming from the parthenogenesis-like reproduction mode. The present  
412 study suggested that reproductive modes significantly affect the intraspecific genetic diversity  
413 of parasites even though they use only a single sedentary host species. Additionally, because  
414 northward colonization events were detected in the phylogenetic study of *Meteterakis* in the

415 Ryukyu and the Japanese Archipelago, this might characterize the phylogeographic histories  
416 of parasites of reptiles in these areas.

417

#### 418 **Declaration of Competing Interests**

419 The authors declare that they have no conflicts of interest.

420

#### 421 **Declaration of funding**

422 This study was supported by the Tokyo Metropolitan University Fund for TMU Strategic  
423 Research (Leader: Professor Noriaki Murakami at TMU; FY2020–FY2022).

424

#### 425 **Acknowledgements**

426 The authors are grateful to T. Makino and Y. Yamane (Kyoto University) for providing host  
427 specimens and to three anonymous reviewers and Dr. Katrine Worsaae (University of  
428 Copenhagen) for their constructive comments and suggestions on the manuscript. We also  
429 thank Elsevier Language Editing Services for editing a draft of this manuscript. Fieldwork in  
430 the Tokara Group was carried out with the permission of Toshima Village.

431

#### 432 **Data Availability Statement**

433 The data that support this study will be shared upon reasonable request to the corresponding  
434 author.

435

#### 436 **References**

- 437 Anderson, R. C. (2000). 'Nematode Parasites of Vertebrates: Their Development and  
438 Transmission,' 2nd edn. (CABI Publishing: Wallingford, UK.)  
439 doi:10.1079/9780851994215.0000
- 440 Badets, M., Whittington, I., Lalubin, F., Allienne, J-F., Maspimby, J-L., Bentz, S., Du Preez,  
441 L. H., Barton, D., Hasegawa, H., Tandon, V., Imkongwapang, R., Ohler, A., Combes, C.,  
442 and Verneau, O. (2011). Correlating early evolution of parasitic platyhelminths to  
443 Gondwana breakup. *Systematic Biology* **60**, 762–731. doi:10.1093/sysbio/syr078
- 444 Baker, M. R. (1980). Revision of *Entomelas* Travassos, 1930 (Nematoda: Rhabdiasidae) with  
445 a review of genera and family. *Systematic Parasitology* **1**, 83–90.  
446 doi:10.1007/BF00009853
- 447 Blasco-Costa, I., and Poulin, R. (2013). Host traits explain the genetic structure of parasites: a  
448 meta-analysis. *Parasitology* **140**, 1316–1322. doi:10.1017/S0031182013000784

449 Bursey, C. R., Goldberg, S. R., and Telford, S. R. (2005). *Plagiorchis taiwanensis* (Digenea:  
450 Plagiorchiidae), *Kurilonema markovi* (Nematoda: Rhabdiasidae) and other helminthes in  
451 *Eumeces latiscutatus* (Scincidae) and *Takydromus tachydromoides* (Lacertidae) from  
452 Japan. *Comparative Parasitology* **72**, 234–240. doi:10.1654/4170

453 Casiraghi, M., Bain, O., Guerrero, R., Martin, C., Pocacqua, V., Gardner, S. L., Franceschi,  
454 A., and Bandi, C. (2004). Mapping the presence of *Wolbachia pipientis* on the phylogeny  
455 of filarial nematodes: evidence for symbiont loss during evolution. *International Journal*  
456 *for Parasitology* **34**, 191–203. doi:10.1016/j.ijpara.2003.10.004

457 Clement, M., Posada, D., and Crandall, K. A. (2000). TCS: a computer program to estimate  
458 gene genealogies. *Molecular Ecology* **9**, 1657–1659. doi:10.1046/j.1365-  
459 294x.2000.01020.x

460 Falk, B. G., and Perkins, S. L. (2013). Host specificity shapes population structure of  
461 pinworm parasites in Caribbean reptiles. *Molecular Ecology* **22**, 4576–4590.  
462 doi:10.1111/mec.12410

463 Furukawa, M., and Fujitani, T. (2014). Comparative study on Pleistocene paleogeographic  
464 maps of Ryukyu Arc. *Bulletin of the Faculty of Science University of the Ryukyus* **98**, 1–8.

465 Greer, A. E., and Shea, G. M. (2000). A major new head scale character in non-lygosomine  
466 scincid lizards. *Journal of Herpetology* **34**, 629–634. doi:10.2307/1565286

467 Hasegawa, H. (1985). Helminth parasites of reptiles from Okinawa, Japan. *The Biological*  
468 *Magazine Okinawa* **23**, 1–11.

469 Hasegawa, H. (1989). *Neoentomelas asatoi* gen. et sp. n. (Nematoda: Rhabdiasidae) and  
470 *Hedruris miyakoensis* sp. n. (Nematoda: Hedruridae) from skinks of the Ryukyu  
471 Archipelago, Japan. *Proceedings of the Helminthological Society of Washington* **56**, 145–  
472 150.

473 Hasegawa, H. (1990). Helminths collected from amphibians and reptiles on Amami-oshima  
474 Island, Japan. *Memoirs of the National Science Museum (Tokyo)* **23**, 83–92.

475 Hasegawa, H. (1992). Parasitic helminths collected from amphibians and reptiles on Kume-  
476 jima Island, Okinawa, Japan. *The Biological Magazine Okinawa* **30**, 7–13.

477 Haukisalmi, V., Hardman, L. M., Fedorov, V. B., Hoberg, E. P., and Henttonen, H. (2016).  
478 Molecular systematics and Holarctic phylogeography of cestodes of the genus  
479 *Anoplocephaloides* Baer, 1923 s. s. (Cyclophyllidae, Anoplocephalidae) in lemmings  
480 (*Lemmus*, *Synaptomys*). *Zoologica Scripta* **45**, 88–102. doi:10.1111/zsc.12136

481 Hasegawa, H., and Iwatsuki, N. (1984). Helminth fauna of tree lizard, *Japarula polygonata* in  
482 Okinawa Prefecture, Japan. *Akamata* **2**, 18–26.

- 483 Ikeda, H., Nishikawa, M., and Sota, T. (2012). Loss of flight promotes beetle diversification.  
484 *Nature Communications* **3**, 648. doi:10.1038/ncomms1659
- 485 Katoh, K., and Standley, D. M. (2013). MAFFT multiple sequence alignment software  
486 version 7: improvements in performance and usability. *Molecular Biology and Evolution*  
487 **30**, 772–780. doi:10.1093/molbev/mst010
- 488 Kisel, Y., and Barraclough, T. G. (2010). Speciation has a spatial scale that depends on levels  
489 of gene flow. *The American Naturalist* **175**, 316–334. doi:10.1086/650369
- 490 Koehler, A. V. A., Hoberg, E. P., Dokuchaev, N. E., Tranbenkova, N. A., Whitman, J. A.,  
491 Nagorsen D. W., and Cook, J. A. (2009). Phylogeography of a Holarctic nematode,  
492 *Soboliphyme baturini*, among mustelids: climate change, episodic colonization, and  
493 diversification in a complex host–parasite system. *Biological Journal of the Linnean*  
494 *Society* **96**, 651–663. doi:10.1111/j.1095-8312.2008.01145.x
- 495 Kuzmin, Y. I., and Sharpilo, V. P. (2002). Rare and locally distributed helminth species of  
496 Palearctic: *Kurilonema markovi* (Nematoda, Rhabdiasidae), the lung parasite of the  
497 Japanese five-lined skink, *Eumeces latiscutatus* (Reptilia, Sauria, Scincidae). *Vestnik*  
498 *Zoologii* **36**, 61–64.
- 499 Kuzmin, Y. I. (2013). Review of Rhabdiasidae (Nematoda) from the Holarctic. *Zootaxa* **3639**,  
500 1–76. doi:10.11646/zootaxa.3639.1.1
- 501 Kuzmin, Y. I., and Tkach, V. V. (2011). Description of a new species of *Kurilonema*  
502 (Nematoda: Rhabdiasidae) from lungs of the skink *Sphenomorphus abdictus aquilonius*  
503 (Reptilia: Squamata: Scincidae) in the Philippines. *Journal of Parasitology* **97**, 506–512.  
504 doi:10.1645/GE-2578.1
- 505 Lanfear, R., Frandsen, P. B., Wright, A. M., Senfeld, T., and Calcott, B. (2017).  
506 PartitionFinder 2: New methods for selecting partitioned models of evolution for molecular  
507 and morphological phylogenetic analyses. *Molecular Biology and Evolution* **34**, 772–773.  
508 doi:10.1093/molbev/msw260
- 509 Leigh, J. W., and Bryant, D. (2015). POPART: full-feature software for haplotype network  
510 construction. *Methods in Ecology and Evolution* **6**, 1110–1116. doi:10.1111/2041-  
511 210X.12410
- 512 Linkem, C. W., Diesmos, A. C., and Brown, R. M. (2011). Molecular systematics of the  
513 Philippine forest skinks (Squamata: Scincidae: *Sphenomorphus*): testing morphological  
514 hypotheses of interspecific relationships. *Zoological Journal of the Linnean Society* **163**,  
515 1217–1243. doi:10.1111/j.1096-3642.2011.00747.x
- 516 Makino, T., Okamoto, T., Kurita, K., Nakano, T., and Hikida, T. (2020). Origin and



517 intraspecific diversification of the scincid lizard *Ateuchosaurus pellopleurus* with  
518 implications for historical island biogeography of the Central Ryukyus of Japan.  
519 *Zoologischer Anzeiger* **288**, 1–10. doi:10.1016/j.jcz.2020.06.008

520 Messing, J. (1983). New M13 vectors for cloning. In ‘Methods in Enzymology Recombinant  
521 DNA, Part C Vol. 101’. (Eds R. Wu, L. Grossman, and K. Moldave.) pp. 20–78.  
522 (Academic Press: New York, USA) doi:10.1016/0076-6879(83)01005-8

523 Minh, B. Q., Schmidt, H. A., Chernomor, O., Schrempf, D., Woodhams, M. D., von Haeseler,  
524 A., and Lanfear, R. (2020). IQ-TREE 2: New models and efficient methods for  
525 phylogenetic inference in the genomic era. *Molecular Biology and Evolution* **37**, 1530–  
526 1534. doi:10.1093/molbev/msaa015

527 Okamoto, T. (2017). Historical biogeography of the terrestrial reptiles of Japan: a comparative  
528 analysis of geographic ranges and molecular phylogenies. In ‘Species Diversity of Animals  
529 in Japan’. (Eds M. Motokawa, and H. Kajihara.) pp. 135–163. (Springer Japan KK: Tokyo,  
530 Japan.) doi:10.1007/978-4-431-56432-4\_5

531 Osozawa, S., Shinjo, R., Armid, A., Watanabe, Y., Horiguchi, T., and Wakabayashi, J. (2012).  
532 Palaeogeographic reconstruction of the 1.55 Ma synchronous isolation of the Ryukyu  
533 islands, Japan, and Taiwan and inflow of the Kuroshio warm current. *International*  
534 *Geology Review* **54**, 1369–1388. doi:10.1080/00206814.2011.639954

535 Ota, H. (1998). Geographic patterns of endemism and speciation in amphibians and reptiles of  
536 the Ryukyu Archipelago, Japan, with special reference to their paleogeographical  
537 implications. *Researches on Population Ecology* **40**, 189–204. doi:10.1007/BF02763404

538 Ota, H., Miyaguni, H., and Hikida, T. (1999). Geographic variation in the endemic skink,  
539 *Ateuchosaurus pellopleurus* from the Ryukyu Archipelago. *Journal of Herpetology* **33**,  
540 106–118. doi:10.2307/1565549

541 Peterson, M. A., and Denno, R. F. (1998). The influence of dispersal and diet breadth on  
542 patterns of genetic isolation by distance in phytophagous insects. *The American Naturalist*  
543 **152**, 428–446. doi:10.1086/286180

544 Prosser, S. W. J., Velarde-Aguilar, M. G., León-Règagnon, V., and Hebert, P. D. N. (2013).  
545 Advancing nematode barcoding: a primer cocktail for the cytochrome c oxidase subunit I  
546 gene from vertebrate parasitic nematodes. *Molecular Ecology Resources* **13**, 1108–1115.  
547 doi:10.1111/1755-0998.12082

548 Pyron, R., Burbrink, F. T., and Wiens, J. J. (2013). A phylogeny and revised classification of  
549 Squamata, including 4161 species of lizards and snakes. *BMC Ecology and Evolution* **13**,  
550 93. doi:10.1186/1471-2148-13-93.

551 Rambaut, A., Drummond, A. J., Xie, D., Baele, G., and Suchard, M. A. (2018). Posterior  
552 summarization in Bayesian phylogenetics using Tracer 1.7. *Systematic Biology* **67**, 901–  
553 904. doi:10.1093/sysbio/syy032

554 Ronquist, F., Teslenko, M., van der Mark, P., Ayres, D. L., Darling, A., Höhna, S., Larget, B.,  
555 Liu, L., Suchard, M. A., and Huelsenbeck, J. P. (2012). MrBayes 3.2: Efficient Bayesian  
556 phylogenetic inference and model choice across a large model space. *Systematic Biology*  
557 **61**, 539–542. doi:10.1093/sysbio/sys029

558 Sands, A. F., Apanaskevich, D. A., Matthee, S., Horak, I. G., and Matthee, C. A. (2017). The  
559 effect of host vicariance and parasite life history on the dispersal of the multi-host  
560 ectoparasite, *Hyalomma truncatum*. *Journal of Biogeography* **44**, 1124–1136.  
561 doi:10.1111/jbi.12948

562 Sata, N. (2015). Distribution of parasitic nematodes in Japan with host–parasite relationship  
563 of lizards of *Plestiodon* (Reptilia:Squamata: Scincidae). *Comparative Parasitology* **82**, 17–  
564 24. doi:10.1654/4728.1

565 Sata, N. (2018). Allopatric speciation of *Meteterakis* (Heterakoidea: Heterakidae), a highly  
566 dispersible parasitic nematode, in the East Asian islands. *Parasitology International* **67**,  
567 493–500. doi:10.1016/j.parint.2018.04.008

568 Shcherbak, N. N., and Sharpilo, V. P. (1969). Data on taxonomy, ecology and parasitology of  
569 reptiles from the Kuril Islands. Communication I. *Vestnik Zoologii* **4**, 18–25.

570 Tamura, K., Peterson, D., Peterson, N., Stecher, G., Nei, M., and Kumar, S. (2011). MEGA5:  
571 molecular evolutionary genetic analysis using maximum likelihood, evolutionary distance,  
572 and maximum parsimony methods. *Molecular Biology and Evolution* **28**, 2731–2739.  
573 doi:10.1093/molbev/msr121

574 Telford, S. R. (1997). ‘The Ecology of a Symbiotic Community. Vol. 1’. (Krieger: Florida,  
575 USA.)

576 Tkach, V. V., Kuzmin, Y. I., and Snyder, S. D. (2014). Molecular insight into systematics, host  
577 associations, life cycles and geographic distribution of the nematode family Rhabdiasidae.  
578 *International Journal for Parasitology* **44**, 273–284. doi:10.1016/j.ijpara.2013.12.005

579 Thompson, J. D., Higgins, D. G., and Gibson, T. J. (1994). CLUSTAL W: improving the  
580 sensitivity of progressive multiple sequence alignment through sequence weighting,  
581 position-specific gap penalties and weight matrix choice. *Nucleic Acids Research* **22**,  
582 4673–4680. doi:10.1093/nar/22.22.4673

583 Wickstöm, L. M., Haukisalmi, V., Varis, S., Hantula, J., Fedorov, V. B., and Henttonen, H.  
584 (2003). Phylogeography of the circumpolar *Paranoplocephala arctica* species complex

585 (Cestoda: Anoplocephalidae) parasitizing collared lemmings (*Dicrostonyx* spp.). *Molecular*  
586 *Ecology* **12**, 3359–3371. doi:10.1046/j.1365-294X.2003.01985.x

587

**Table 1. Number of specimens and genetic composition of each sampling locality examined in this study**

588

The H6 sequence marked with an asterisk (\*) was distinguished from the ‘true’ H6 by a single indel-derived polymorphism

Locality no.	Locality name	Island group	<i>n</i> (mtDNA)	Haplotype (mtDNA)	<i>n</i> (18S–28S)	Haplotype (18S–28S)
1	Takeshima Island, Kagoshima	Mishima Islands	1	M1	n/a	n/a
2	Iojima Island, Kagoshima	Mishima Islands	5	M1, M2	3	H2
3	Suwanosejima Island, Kagoshima	Tokara Islands	3	T1	3	H1
4	Kodakarajima Island, Kagoshima	Tokara Islands	4	T2, T3	1	H6*
5	Amami City, Amamioshima Island, Kagoshima	Amami Islands	11	Aa1, Aa2, Aa3, Aa4, Aa5	6	H6
6	Yamato Village, Amamioshima Island, Kagoshima	Amami Islands	13	Ay1, Ay2, Ay3, Ay4, Ay5, Ay6, Ay7, Ay8, Ay9	7	H6
7	Tokunoshima Town, Tokunoshima Island, Kagoshima	Amami Islands	6	Tku1	5	H4, H5
8	Isen Town, Tokunoshima Island, Kagoshima	Amami Islands	1	Tku2	1	H4
9	Iheyajima Island, Okinawa	Okinawa Islands	7	I1, I2, I3, I4	5	H6
10	Ogimi Village, Okinawajima Island, Okinawa	Okinawa Islands	6	O1, O2, O3	4	H3, H6
11	Hamahigajima Island, Okinawa	Okinawa Islands	5	Hm1	2	H8
12	Tokashikijima Island, Okinawa	Okinawa Islands	3	Tka1, Tka2	3	H8
13	Kumejima Island, Okinawa	Okinawa Islands	9	K1, K2, K3, K4 K5, K6	7	H7, H8

589

590 **FIGURE LEGENDS**

591

592 **Fig. 1.** Map of the Ryukyu Archipelago. (A) The entire studied area in the Ryukyu  
593 Archipelago; (B) sampling localities in the Ryukyu Archipelago. The locality numbers are  
594 consistent with those in Table 1.

595

596 **Fig. 2.** A Bayesian phylogenetic tree for rhabdiasid nematodes based on the nuclear *18S–28S*  
597 marker. The numbers on branches represent Bayesian posterior probabilities and bootstrap  
598 values for maximum likelihood.

599

600 **Fig. 3.** A Bayesian intraspecific phylogenetic tree for *Neoentomelas asatoi* based on  
601 mitochondrial markers. The numbers on branches represent Bayesian posterior probabilities  
602 and bootstrap values for maximum likelihood. The details of haplotype numbers are listed in  
603 Table 1. Vertical white bars indicate the Okinawa Islands' subclades, single gray bars indicate  
604 the Northern Ryukyus' and southern Tokara Islands' subclades, and black bars indicate the  
605 Amami Islands' subclades.

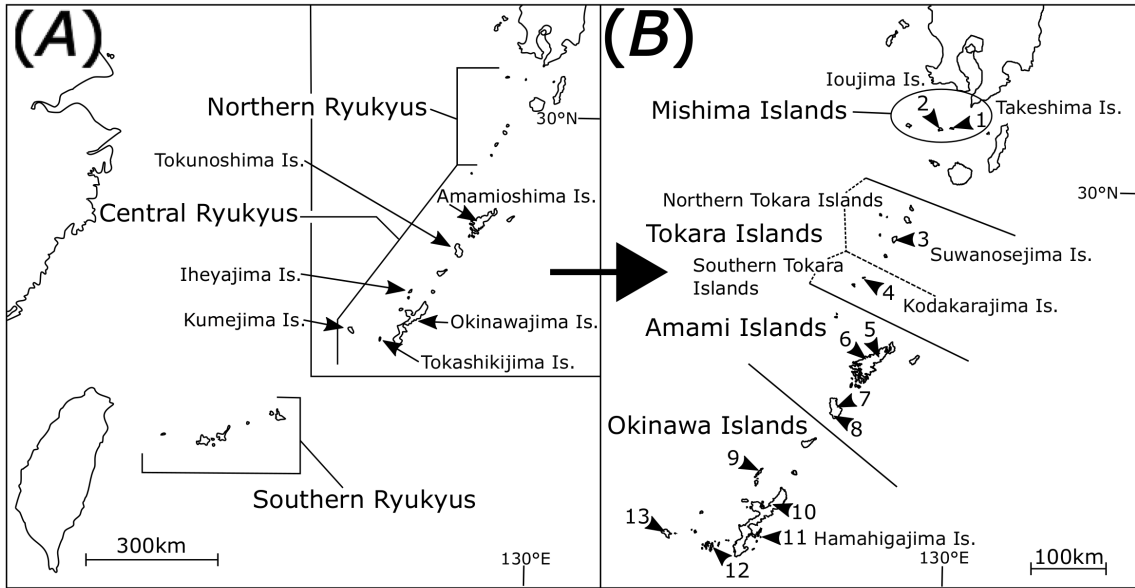
606

607 **Fig. 4.** Statistical parsimony network for the *18S–28S* haplotypes of *Neoentomelas asatoi*.  
608 The details of haplotype numbers are listed in Table 1.

609

610 **Fig. 5.** The geological distribution of the mitochondrial haplotypes of *Neoentomelas asatoi*.  
611 The ingroup phylogenetic tree is identical to that in Fig. 3. The details of haplotype numbers  
612 are listed in Table 1. Arrows indicate colonization events of *N. asatoi*. Solid circles on the  
613 phylogenetic tree and arrows indicate the colonization events from Iheyajima Island to  
614 Amamioshima Island, and solid star shapes indicate the colonization events among  
615 Okinawajima Island, Kodakarajima Island and Suwanosejima Island. Dotted lines indicate the  
616 geological distribution of two major clades of the host lizard (*Ateuchosaurus pellopleurus*),  
617 Clade Ok: a clade comprising the populations in the Okinawa Islands; Clade A + NR: a clade  
618 comprising the populations in the Amami Islands and northern Ryukyu.

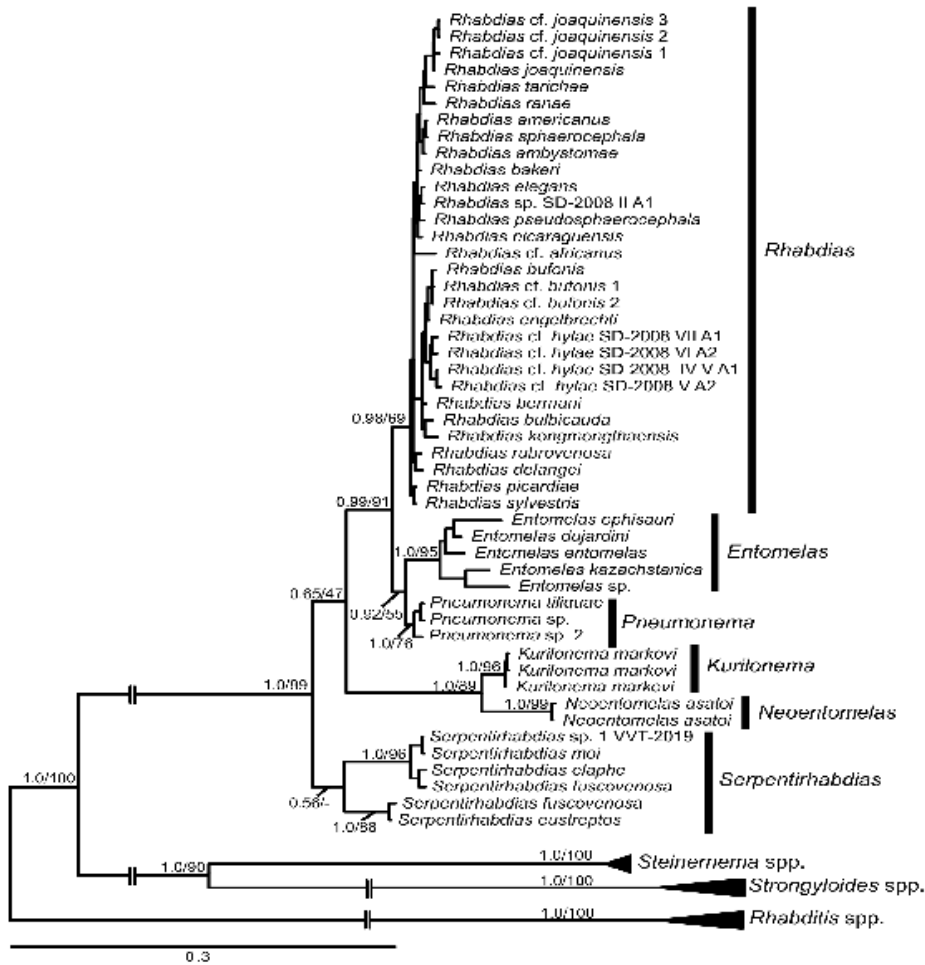
619



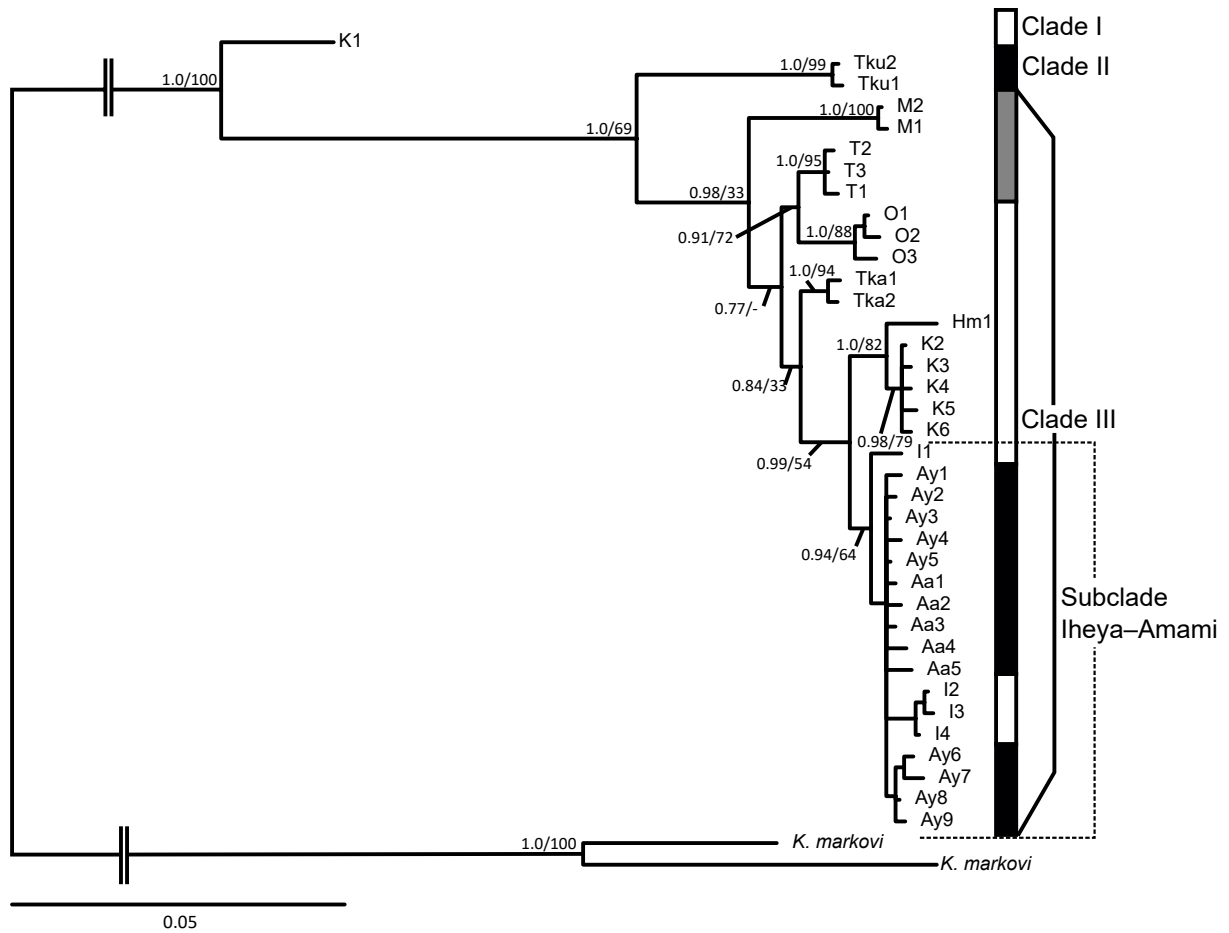
620

621 **Fig. 1.** Map of the Ryukyu Archipelago. (A) The entire studied area in the Ryukyu  
 622 Archipelago; (B) sampling localities in the Ryukyu Archipelago. The locality numbers are  
 623 consistent with those in Table 1.

624



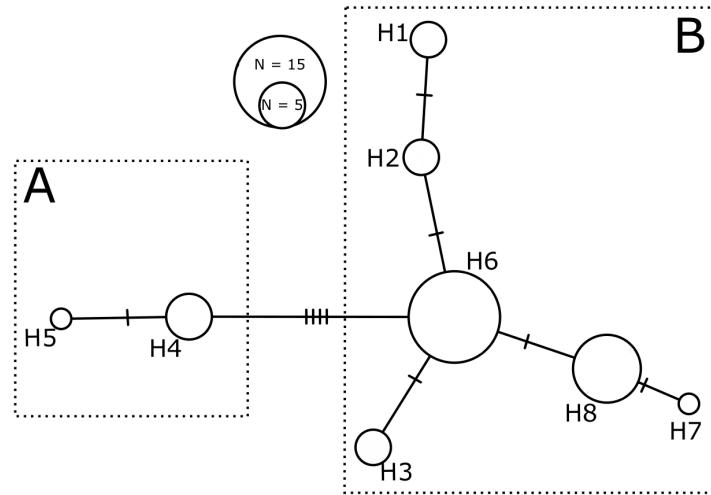
625  
 626 **Fig. 2.** A Bayesian phylogenetic tree for rhabdiasid nematodes based on the nuclear *18S–28S*  
 627 marker. The numbers on branches represent Bayesian posterior probabilities and bootstrap  
 628 values for maximum likelihood.  
 629



630  
 631  
 632  
 633  
 634  
 635  
 636  
 637

**Fig. 3.** A Bayesian intraspecific phylogenetic tree for *Neotentomelas asatoi* based on mitochondrial markers. The numbers on branches represent Bayesian posterior probabilities and bootstrap values for maximum likelihood. The details of haplotype numbers are listed in Table 1. Vertical white bars indicate the Okinawa Islands' subclades, single gray bars indicate the Northern Ryukyus' and southern Tokara Islands' subclades, and black bars indicate the Amami Islands' subclades.



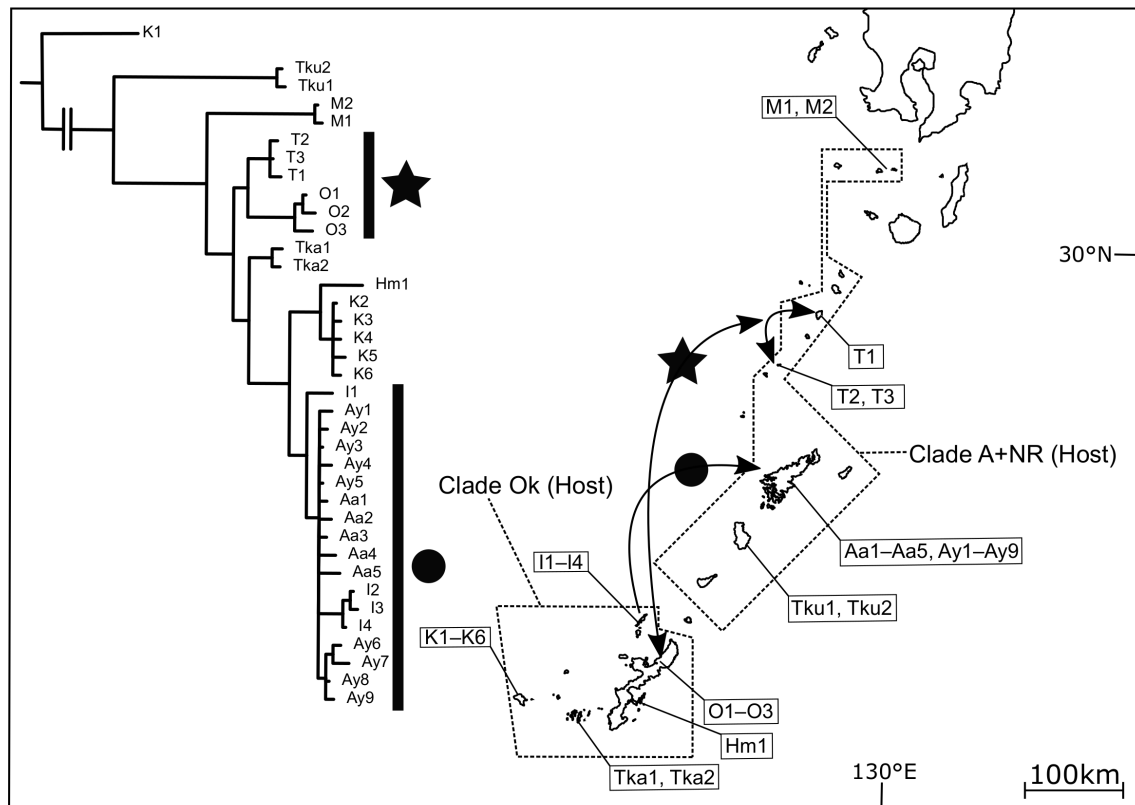


638

639 **Fig. 4.** Statistical parsimony network for the 18S–28S haplotypes of *Neoentomelas asatoi*.

640 The details of haplotype numbers are listed in Table 1.

641



642  
 643 **Fig. 5.** The geographical distribution of the mitochondrial haplotypes of *Neoentomelas asatoi*.  
 644 The ingroup phylogenetic tree is identical to that in Fig. 3. The details of haplotype numbers  
 645 are listed in Table 1. Arrows indicate colonization events of *N. asatoi*. Solid circles on the  
 646 phylogenetic tree and arrows indicate the colonization events from Iheyajima Island to  
 647 Amamioshima Island, and solid star shapes indicate the colonization events among  
 648 Okinawajima Island, Kodakarajima Island and Suwanosejima Island. Dotted lines indicate the  
 649 geographical distribution of two major clades of the host lizard (*Ateuchosaurus pellopleurus*),  
 650 Clade Ok: a clade comprising the populations in the Okinawa Islands; Clade A + NR: a clade  
 651 comprising the populations in the Amami Islands and northern Ryukyus.